Supplemental Figure 1. ARdNLS24Q male mice display no rotarod deficit. Latency to fall from an accelerating rotarod was measured every 4 weeks from 8 to 28 weeks of age in a large cohort of mice. *n*=15 (non-transgenic and ARdNLS24Q).

Supplemental Figure 2. ARdNLS does not cause inhibition of weight gain in mice. Weights were measured for a large cohort of mice every 4 weeks from 8 to 28 weeks of age. AR112Q (*n*=10) and ARdNLS112Q (*n*=15) males **(*A*)** *=p ≤ 0.05 between AR112Q males and non-transgenic (*n*=15) males, female ARdNLS112Q (*n*=10) mice **(*B*)** *=p ≤ 0.05 between AR112Q females and non-transgenic females (*n*=15), ARdNLS24Q males **(*C*)**. Significance was determined using two-way ANOVA.

Supplemental Figure 3. Analysis of AR aggregation in brain. ***A,*** Cortical neurons from 8, 16 and 24 week old mice immunostained for AR (ARH280) and stained with Hoechst to reveal nuclei. ***B,*** Protein lysates from the brains as in ***A*** were prepared to evaluate oligomeric species of AR (AR(N-20)) by western blot. NS = non-specific bands.

Supplemental Figure 4. In brain, ARdNLS112Q is detected within the cytoplasmic fraction to a greater extent than the nuclear fraction. Fresh brain and thoracic sacral spinal cord were fractionated according to Pierce protocol (78833). One brain hemisphere and the cervical section of the spinal cord were flash frozen, pulverized and homogenized in 10 volumes of Trion-DOC lysis buffer for total protein. One-hundred and sixty micrograms of total protein, 320 ug cytoplasmic fraction and 8 times the cellular equivalent of the nuclear fraction were loaded (noted as (8x)), onto a 10% gel and western analyzed for AR, GAPDH and HMBG1.

Supplemental Figure 5. ARdNLS24Q accumulates within nuclei and does not form intranuclear inclusions. Images shown are of cortical neurons from a 37-week-old ARdNLS24Q male mouse immunostained for AR (ARH280) and stained with Hoechst to reveal nuclei.

Supplemental Figure 1

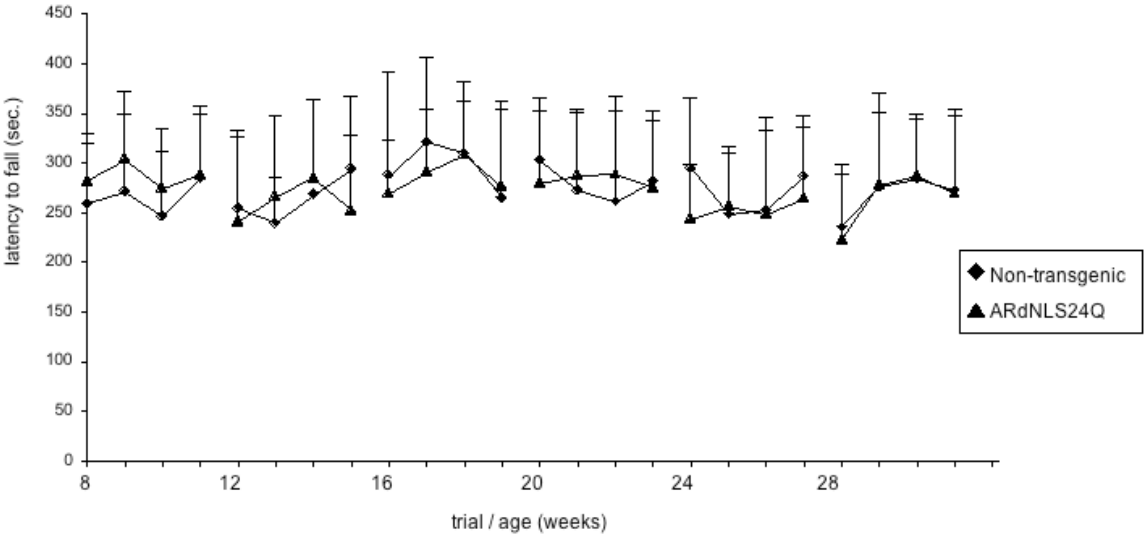

Supplemental Figure 2

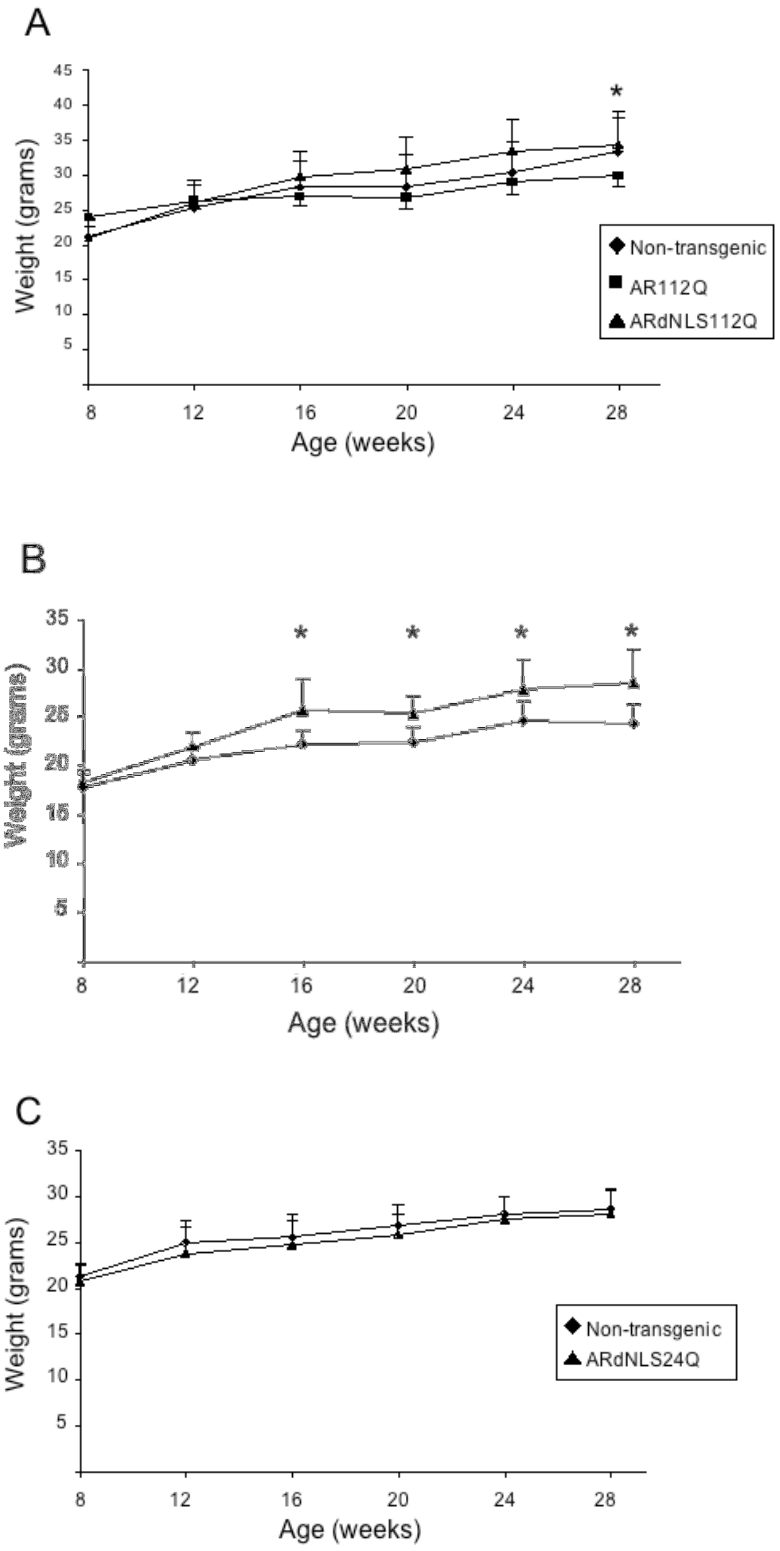

Supplemental Figure 3

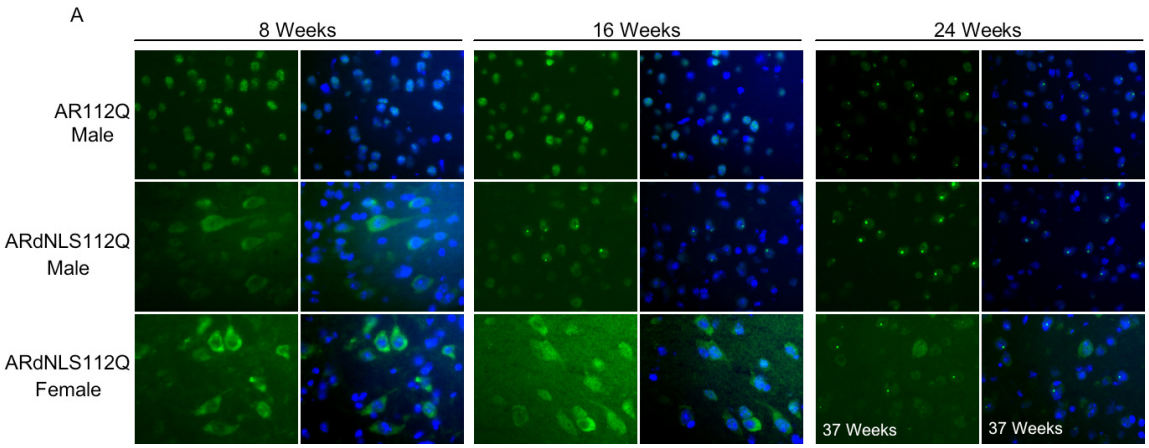

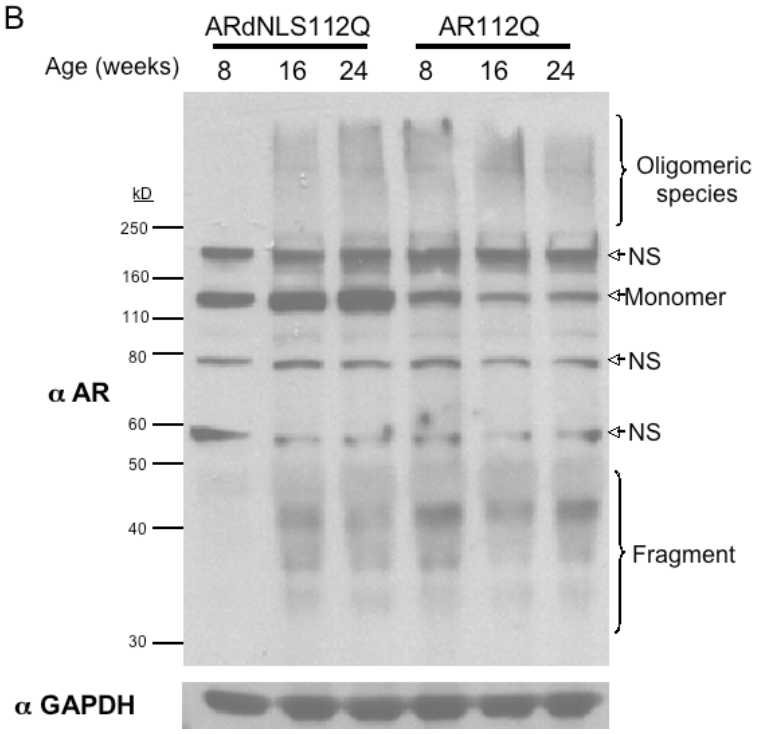

Supplemental Figure 4

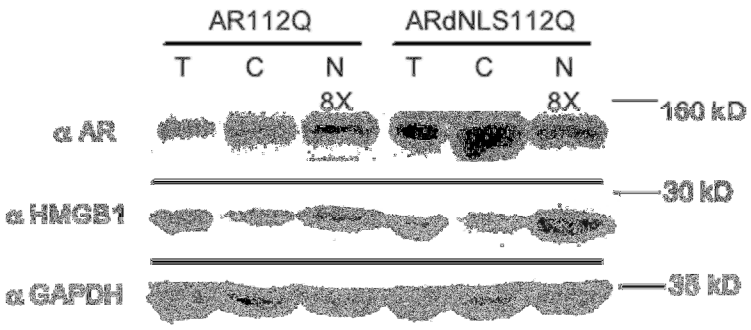

Supplemental Figure 5